AIP | Physics of Plasmas

# Effects of the frequency detuning in Raman backscattering of infinitely long laser pulses in plasmas

Min Sup Hur, Ilmoon Hwang, Hyo Jae Jang, and Hyyong Suk

Citation: Physics of Plasmas (1994-present) **13**, 073103 (2006); doi: 10.1063/1.2222327

View online: http://dx.doi.org/10.1063/1.2222327

View Table of Contents: http://scitation.aip.org/content/aip/journal/pop/13/7?ver=pdfcov

Published by the AIP Publishing

# Effects of the frequency detuning in Raman backscattering of infinitely long laser pulses in plasmas

Min Sup Hur and Ilmoon Hwang
*Center for Advanced Accelerators, KERI, Changwon, Kyongnam 641-120, Korea*

Hyo Jae Jang
*Center for Advanced Accelerators, KERI, Changwon, Kyongnam 641-120, Korea*
*and Department of Physics, POSTECH, Kyongbuk 790-784, Korea*

Hyyong Suk[a)]
*Center for Advanced Accelerators, KERI, Changwon, Kyongnam 641-120, Korea*

(Received 27 April 2006; accepted 21 June 2006; published online 25 July 2006)

Raman backscattering (RBS) in an infinite homogeneous laser-plasma system was investigated with the three-wave fluid model and averaged particle-in-cell (aPIC) simulations in the nonrelativistic and low temperature regime. It was found that the periodic boundary condition for the electrostatic potential, which is commonly used in an infinite homogeneous plasma, induces a numerical frequency shift of the plasma wave. The initial frequency detuning between the three waves is modified by the frequency shift, leading to a significantly wrong result in the RBS system. An alternative boundary condition based on the Maxwell equation is presented. The aPIC simulations with the modified boundary condition show that the pump depletion level depends sensitively on the frequency mismatch between the three waves. This sensitivity is closely related with the erroneous RBS: the numerical frequency shift is very minor (a few percent of the plasma frequency or less than that) but RBS can be greatly affected even by such a small frequency change. Analytic formulas for the pump depletion time and level is derived and compared to the aPIC simulations with the modified boundary condition, showing an excellent agreement. © *2006 American Institute of Physics*. [DOI: 10.1063/1.2222327]

## I. INTRODUCTION

Raman scattering of laser pulses in a plasma is an important physical process in laser-plasma systems and their applications. Spectroscopy utilizing Raman scattering[1–3] is a powerful diagnostic of the plasma density and plasma wave amplitude (by coupling with Thomson scattering). Unexpectedly high Raman backscattering was one of the major obstacles to the fast ignition in the inertial fusion, which motivated a series of intensive experimental, theoretical, and numerical studies of Raman backscattering (RBS).[4,5] Recently a novel scheme of the laser pulse amplification [Raman backward amplification (RBA)] using RBS has been proposed[6] and intensively studied theoretically and experimentally.[7,8] Among the important issues in RBS there are kinetic effects such as electron trapping and Landau damping. From the reduced particle-in-cell simulations and analysis, it was found that electron trapping enhances RBS over the naive prediction based on the linear Landau damping theory in a high temperature plasma.[4] A kinetic term which describes the trapping effect was found by Hur *et al.*[9] From the analysis of the kinetic term, it was shown that the trapping suppresses RBS in a low temperature plasma, where the linear Landau damping is negligible. This effect is important in RBA as the efficiency of the amplification can be significantly deteriorated in some parameter regimes.[9,10]

In this article, we focus on the spatially homogeneous RBS in a nontrapping regime, which was not covered in previous work.[9] Using the averaged particle-in-cell (aPIC) simulation[11] and a simple analytic theory, the effects of the initial pump and seed amplitudes and the frequency mismatch are studied. The homogeneous RBS, where the spatial modulation is neglected, can frequently occur when a very long laser pulse propagates through a plasma. For a long pump laser, Raman backscattering is more dominant than other instabilities such as Raman forward scattering or the modulation because of its higher growth rate. Thus, it is important to investigate the characteristics of the homogeneous RBS. The most popular model for the homogeneous RBS is the three-wave equations without spatial derivatives, which have been investigated analytically.[12–14] Those equations can be used to describe interactions between light waves and general dielectric materials, not only the plasma.[13] However, in the previous works[9–11] and other literatures,[15,16] it was shown that the three-wave model is not valid in the kinetic regime where particle trapping and wave breaking are involved. Even below the wave-breaking limit, the kinetic approach is important because RBS is, as it turns out, extremely sensitive to any possible detuning mechanism which is not included self-consistently in the three-wave model. In this article, we address the homogeneous RBS by the aPIC simulations,[11] focusing on the effect of frequency detuning between the three waves. The simulations show that a very small frequency mismatching leads to a significant change in the pump depletion level. It will be shown that RBS characteristics are seriously distorted when the common periodic

[a)]Electronic mail: hysuk@keri.re.kr

 

boundary condition of the electrostatic potential is used in the PIC simulations because of the unrealistic frequency shift induced by the (numerical) Doppler shift. The erroneous frequency shift was pointed out theoretically for the beat-wave-driven plasma wave.[17,18] In that system, the relativistic mass increase is the origin of the frequency shift. In RBS, the operation regime is nonrelativistic (no relativistic frequency shift) and RBS can be easily affected by any small frequency mismatch. Thus, it is important to study the issue with first-principle simulations (i.e., PIC simulations). The analytic forms of the pump depletion time and level were compared with a series of aPIC[11] simulations.

This article is organized as follows: The basic equations of the aPIC model are reviewed in Sec. II with a useful discussion on the boundary condition of the electrostatic potential. The RBS simulations and analysis are presented in Sec. III. The summary is given in Sec. IV.

## II. THE AVERAGED PARTICLE-IN-CELL MODEL FOR RBS

The kinetic effects on RBS can be modeled self-consistently by PIC simulations. However, full PIC codes, which solve the Maxwell equations and the equation of motion for plasma particles, are computationally expensive. As a compromise of the PIC's self-consistency in describing the kinetic features and the fast computation of the three-wave fluid model, Shvets *et al.* used the envelope-kinetic model, where he studied for the first time the laser amplification in a highly kinetic regime.[19,20] That concept was extended to the aPIC code,[11] which couples the envelope-kinetic equations of the lasers with the conventional PIC scheme for plasmas.

### A. Basic equations

The spatially homogeneous version of the envelope-kinetic equations for lasers used in Refs. 11 and 20 are

$$\frac{da_1}{dt} = i\frac{\omega_p^2}{2\omega_1}a_2\left\langle \frac{e^{i\phi_j}}{\gamma_j}\right\rangle, \tag{1a}$$

$$\frac{da_2}{dt} = i\frac{\omega_p^2}{2\omega_2}a_1\left\langle \frac{e^{-i\phi_j}}{\gamma_j}\right\rangle, \tag{1b}$$

where $a_{1,2}$ are the seed and the pump envelopes, $\omega_1 \simeq \omega_2$ the frequencies of the seed and the pump, and $\phi_j$ the ponderomotive phase of the $j$th particle. For the system to be nonkinetic, no electron trapping or wave breaking should occur and the driving laser amplitude should be small, i.e., $a_{1,2} \ll 1$. To keep the plasma wave amplitude under the wave-breaking limit, every particle's velocity should be less than the phase velocity $v_p$ of the plasma wave. The plasma wave is driven by the beat of the two counterpropagating lasers with $(\omega_{1,2}, k_{1,2})$. Thus $v_p$ for nearly resonant frequency matching $(\omega_2 - \omega_1 \simeq \omega_p)$ is given by $v_p/c = (\omega_2 - \omega_1)/c(k_1 + k_2) \simeq \omega_p/2\omega$, where $\omega = (\omega_1 + \omega_2)/2$. A typical value of $\omega_p/\omega$ for a tenuous plasma is less than 0.1. Therefore, as long as the driving lasers are weak enough to keep the plasma wave amplitude under the wave-breaking limit, all the electrons are nonrelativistic. Hence, the relativistic factor in Eq. (1) can be removed.

The electrostatic plasma wave is treated in an exactly same way as in the conventional electrostatic PIC codes. The spatially homogeneous equation of motion for the $j$th electron is

$$\frac{du_j}{dt} = -\frac{e}{mc}E_s + \frac{ck_b}{2}\Re\mathrm{e}[ia_1^* a_2 e^{i\phi_j}], \tag{2}$$

where $u_j = \gamma_j v_j/c \simeq v_j/c$, $k_b$ the beat wave number, and $E_s$ the electrostatic field. To obtain $E_s$, the simulation domain (typically one beat wavelength) is divided into meshes, to which the charge from the simulation particles is allocated with some weighting (we used linear weighting). The ions are assumed to be fixed in the time scale of RBS.

### B. Boundary condition

The one-dimensional electric field can be obtained from the Poisson equation ($\partial_x^2\phi = -\rho/\epsilon_0$, $-\partial_x\phi = E$). In an infinite homogeneous system, the periodic boundary condition is commonly used for the electric potential, which enforces the spatial dc component of the electric field to disappear. In principle, however, there is no physical mechanism prohibiting the temporally alternating dc electric field. On the contrary, the time-varying dc electric field is essential to cancel any spatially constant current induced by noise or any external driving. Otherwise, the system cannot satisfy the Maxwell equation

$$\epsilon_0\frac{\partial E_\mathrm{x}}{\partial t} + J_\mathrm{x} = 0. \tag{3}$$

This was pointed out previously in another context[18] without detailed description on the numerical boundary condition or evidences from PIC simulations. We present the numerical condition for the electric field, which satisfies Eq. (3). The infinite homogeneous system can be simulated by considering just one wavelength of the plasma wave. The motion of particles and the electric field are periodically repeated. The wavelength is divided by $N$ meshes and the discretized plasma densities $n_j$'s are computed on the grid points from the simulation particles with a proper weighting (linear weighting was used in our simulations). Then the electric field $E_{j+1/2}$ is calculated at the center of the meshes from

$$E_{j+1/2} - E_{j-1/2} = -\frac{en_j}{\epsilon_0}\Delta x, \tag{4}$$

where $\Delta x$ is the mesh size. To close Eq. (4), either the boundary value, $E_{1/2}$ or $E_{N-1/2}$, should be specified. The spatial dc component of any discretized quantity $Q_j$ is represented by $Q_\mathrm{dc} = (1/N)\Sigma_{j=0}^{N-1} Q_j$. This equation along with Eq. (4) gives

$$E_\mathrm{dc} = \sum_{j=0}^{N-1} E_{j+1/2} = E_{N-1/2} + \frac{e\Delta x}{\epsilon_0 N}\sum_{j=1}^{N-1} jn_j. \tag{5}$$

The electron current at each simulation grid can be obtained by counting the number of particles passing through a given mesh boundary divided by the simulation time step;

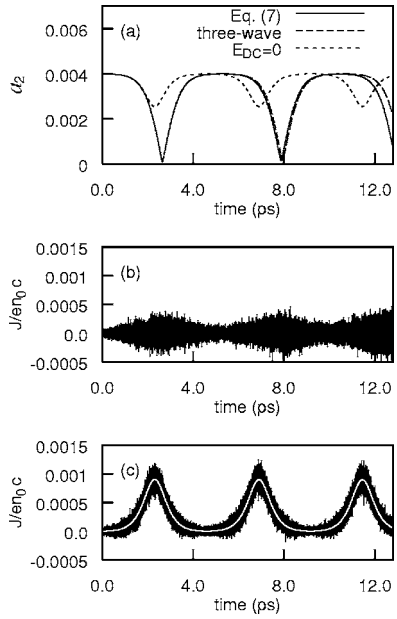


FIG. 1. (a) Comparison of the aPIC simulations with Eq. (7) (i.e., $J_{dc}=0$, solid line) and with $E_{dc}=0$ (dotted line). The three-wave fluid calculation (dashed line) is shown to be in a good agreement with the $J_{dc}=0$ case. (b and c) dc components in the current for $J_{dc}=0$ and $E_{dc}=0$, respectively.

the sign of the current from each electron is opposite to that of the particle velocity. The time-discrete version of Eq. (3) for the dc components becomes

$$E_{\mathrm{dc}}^{n} = E_{\mathrm{dc}}^{o} - \frac{\Delta t}{\epsilon_0} J_{\mathrm{dc}}^{o}, \tag{6}$$

where the superscripts $n, o$ represent the new and old steps in time. From Eqs. (5) and (6), the boundary value $E_b \equiv E_{N-1/2}$ is determined by

$$E_b^{n} = E_{\mathrm{dc}}^{o} - \frac{\Delta t}{\epsilon_0} J_{\mathrm{dc}}^{o} - \frac{e\Delta x}{\epsilon_0 N} \sum_{j=1}^{N-1} j n_j^{n}. \tag{7}$$

Note that periodic boundary condition for the electric potential means $E_{\mathrm{dc}}=0$ in Eq. (5).

We discuss the discrepancy between two aPIC simulations with different boundary conditions. Figure 1(a) is the comparison between the aPIC simulation with the boundary condition from Eq. (7) and the periodic potential, i.e., $E_{\mathrm{dc}}=0$. To confirm that the former produced a correct result, the dc components of the electron current density were compared for those two cases in Figs. 1(b) and 1(c). The dc current density was well suppressed by the induced dc electric field when Eq. (7) was used as a boundary condition, whereas it was not in the other case. The aPIC with Eq. (7) agrees well with the three-wave fluid calculation. The three-wave equations and analysis will be given in the next section.

The dc current in Fig. 1(c) originates from the coupling between the linear perturbations in the plasma density $(n_1)$ and the fluid velocity $(v_1)$. These quantities are represented by

$$n_1 = \tfrac{1}{2}[\hat{n}_1 \exp(ikx - i\omega t) + \text{c.c.}], \tag{8a}$$

$$v_1 = \tfrac{1}{2}[\hat{v}_1 \exp(ikx - i\omega t) + \text{c.c.}]. \tag{8b}$$

The Poisson equation and the fluid equation of motion give the complex amplitudes $\hat{n}_1$ and $\hat{v}_1$ as functions of the electric field amplitude:

$$\frac{\hat{n}_1}{n_0} = -i\frac{ck}{\omega_p} f, \quad \hat{v}_1 = -icf, \tag{9}$$

where $f$ is the first-order complex amplitude of the electric field normalized by $f = eE/m_e\omega_p c$ and $n_0$ is the unperturbed plasma density. The second order current is calculated as

$$\frac{J_2}{en_0 c} = -\frac{v_2}{c} - \frac{n_1 v_1}{n_0 c}. \tag{10}$$

The second term in Eq. (10), from Eqs. (8) and (9), yields a spatial dc current as well as an oscillatory component:

$$\frac{J_2}{en_0 c} = -\frac{v_2}{c} + \frac{ck}{4\omega_p} f^2 \exp(2ikx - 2i\omega t) + \text{c.c.} - \frac{ck}{2\omega_p}|f|^2. \tag{11}$$

The white line in Fig. 1(c) is the plot of the last term in Eq. (11), which exactly overlaps on the measured current. The dc current from the coupling of $n_1$ and $v_1$ should be canceled by another dc term originating from the second-order drift $v_d/c = 0.5ck|f|^2/\omega_p$ of the fluid plasma.[17,18] However, when the boundary condition of $E_{\mathrm{dc}}=0$ is used, there is no driving to invoke $v_d$. To satisfy the Maxwell equation (3), the PIC simulation will take an alternative way: the moving frame with a velocity $-v_d$. In this frame, the ion background will generate a current which cancels the dc term in Eq. (11). In the PIC simulation, there is no distinction between the moving and fixed ion backgrounds, because, as long as there is no spatial modulation in the ion density, the moving ions do not make any change in solving the Poisson equation. Thus the cancelling ion current intervenes only implicitly. Instead, taking a moving frame results in an unrealistic frequency change by the Doppler shift. Because the frame will move in a way to cancel the last term in Eq. (11), the shift becomes $\Delta\omega/\omega_p = kv_d/\omega_p = c^2k^2|f|^2/2\omega_p^2$. The (numerical) frequency change is always up-shift and depends on the square of the wave amplitude. This frequency shift is a major source of the significant discrepancy in Fig. 1. Note that a small frequency mismatch can lead to a great difference in the pump depletion level as will be shown in the next section (Fig. 2).

## III. SIMULATION RESULTS AND ANALYSIS

We used two different types of simulations: averaged PIC simulation, which includes every kinetic feature self-consistently, and the three-wave fluid model. The aPIC scheme is presented in the previous section. The governing equations of the fluid three-wave model are

$$\frac{\partial a_1}{\partial t} + c\frac{\partial a_1}{\partial x} = -\frac{\omega_p}{2} a_2 f^*, \tag{12a}$$

$$\frac{\partial a_2}{\partial t} - c\frac{\partial a_2}{\partial x} = \frac{\omega_p}{2} a_1 f, \tag{12b}$$

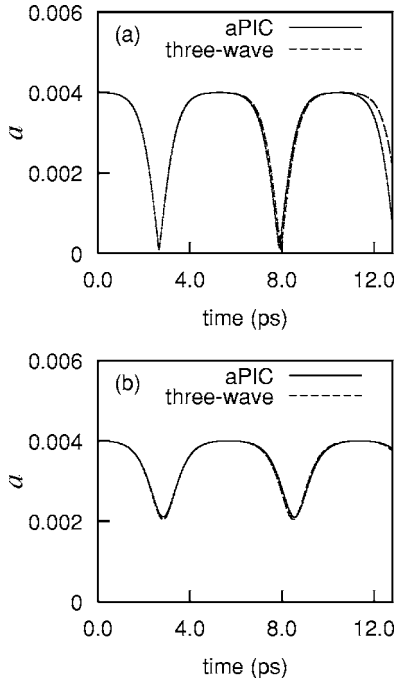


FIG. 2. The temporal evolution of the pump envelopes for (a) resonant case and (b) slightly off-resonant case ($\delta\omega/\omega_p$ is less than 1%). The solid lines are from kinetic simulations using aPIC, and the dashed lines are from the three-wave fluid model.

$$\frac{\partial f}{\partial t} + i\delta\omega f + \frac{3}{2}\frac{k_b^2 T_e}{m_e \omega_p} f = -\frac{\omega}{2} a_1^* a_2, \tag{12c}$$

where $f$ is the envelope of the plasma wave, $\delta\omega = \omega_p - \omega_2 + \omega_1$, $T_e$ the plasma temperature, $k_b$ the beat wave number of the two counterpropagating lasers, $m_e$ the electron rest mass, and $\omega = (\omega_1 + \omega_2)/2$. It will be discussed that the plasma temperature has a nonnegligible effect on RBS. Note that the spatial derivatives in Eq. (12) are neglected in an infinite homogeneous system.

Figure 2 shows the homogeneous RBS obtained from the three-wave fluid and aPIC simulations. The initial amplitudes of the seed and pump were $a_1 = 0.0005$ and $a_2 = 0.004$, respectively. The wavelengths were $\lambda_1 = 1.0\ \mu$m and $\lambda_2 = 0.9\ \mu$m. Two different plasma densities were used: $n = 1.379 \times 10^{19}$ and $n = 1.362 \times 10^{19}\ \text{cm}^{-3}$, corresponding to plasma frequencies of $\omega_p = 2.092 \times 10^{14}$ and $\omega_p = 2.079 \times 10^{14}$, respectively. The former satisfies the resonance condition between the lasers and plasma ($\delta\omega = 0$) and the latter is slightly off-resonant by 0.7% ($|\delta\omega|/\omega_p = 0.007$). For the exact resonant case, the pump is depleted by almost 100%. The slightly off-resonant case, though the initial growth rate of the seed laser is almost the same as in the resonant case, the level of the pump depletion is quite different. The pump depletion level in the off-resonant case is similar to that from the aPIC simulation with resonance but a wrong boundary condition ($E_{\text{dc}} = 0$ case in Fig. 1). Note that the middle value of the numerical frequency shift in Fig. 1(c) is approximately $\Delta\omega/\omega_p \sim 0.0005ck/\omega_p \simeq 0.01$ (1%), which is similar to the detuning used in Fig. 2(b). After the energy depletion, the pump begins to get back the energy from the seed and plasma wave. The energy depletion and restoration procedure is repeated.

We investigate the effect of the detuning and the laser intensities on the pump depletion time and depletion level. To do this, it is useful to decompose the laser and plasma envelopes in Eq. (12) into their (positive) magnitudes and phases as $a_{1,2} = \tilde{a}_{1,2} \exp(i\theta_{1,2})$ and $f = \tilde{f} \exp(i\theta_f)$. Substituting these into Eq. (12) and neglecting the spatial derivative terms (due to the infinite homogeneity) yield the magnitude equation

$$\frac{d\tilde{a}_1}{dt} = -\frac{\omega_p}{2}\tilde{a}_2\tilde{f}\cos\theta, \tag{13a}$$

$$\frac{d\tilde{a}_2}{dt} = \frac{\omega_p}{2}\tilde{a}_1\tilde{f}\cos\theta, \tag{13b}$$

$$\frac{d\tilde{f}}{dt} = -\frac{\omega}{2}\tilde{a}_1\tilde{a}_2\cos\theta, \tag{13c}$$

and the phase equation

$$\frac{d\theta}{dt} = K\sin\theta - \delta\omega, \tag{14}$$

where $\theta = \theta_f + \theta_1 - \theta_2$ is the relative phase. In Eq. (14), $K$ is defined by

$$K = \frac{\omega}{2}\frac{\tilde{a}_1\tilde{a}_2}{\tilde{f}} + \frac{\omega_p}{2}\frac{\tilde{a}_2\tilde{f}}{\tilde{a}_1} - \frac{\omega_p}{2}\frac{\tilde{a}_1\tilde{f}}{\tilde{a}_2}. \tag{15}$$

Multiplying $\tilde{a}_1$ and $\tilde{a}_2$ to Eqs. (13a) and (13b) and summing those two equations yield

$$\tilde{a}_1^2 + \tilde{a}_2^2 = \tilde{a}_{10}^2 + \tilde{a}_{20}^2, \tag{16}$$

where $\tilde{a}_{10,20}$ represent initial amplitudes of the seed and pump. By applying the same procedure to Eqs. (13b) and (13c), $\tilde{f}$ can be represented by $\tilde{a}_2$:

$$\tilde{a}_2^2 + \frac{\omega_p}{\omega}\tilde{f}^2 = \tilde{a}_{20}^2. \tag{17}$$

The plasma wave starts from zero amplitude $\tilde{f} = 0$. Thus the value of $K$ at $t = 0$ is $\infty$, from which the relative phase $\theta$ takes a stable equilibrium at $\theta = \pi$. Until $K$ changes its sign, $\theta$ remains there, where the driving of the pump ($\propto \cos\theta$) is negative. Therefore pump energy is being transferred to the seed and the plasma wave. As $\tilde{a}_2$ becomes small, the negative term in $K$ becomes dominant eventually flipping the sign of $K$. Even after $K$ changes its sign, the driving of the pump still remains negative for some time, as it takes long for $\theta$ to leave its original position to a new stable equilibrium (either 0 or $2\pi$). Thus we roughly assume that $\theta$ stays at $\pi$ until the pump is completely depleted. From aPIC simulations, this assumption could be found to be quite valid. From Eqs. (13b), (16), and (17), and $\theta = \pi$, the equation of the temporal evolution of $\tilde{a}_2$ can be obtained as follows:

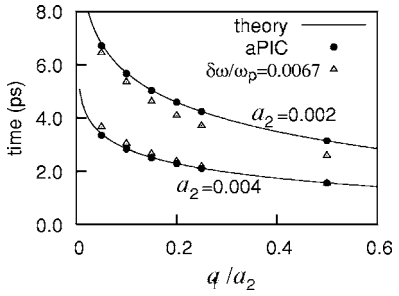


FIG. 3. Pump depletion time as a function of the initial seed and pump ratio $(a_1/a_2)$ for two different pump intensities, $a_2=0.002$ and $a_2=0.004$.

$$\frac{d\chi}{dt} = -\tilde{a}_{20}\frac{\sqrt{\omega_p\omega}}{2}\sqrt{1+\nu^2-\chi^2}\sqrt{1-\chi^2}, \tag{18}$$

where $\chi=\tilde{a}_2/\tilde{a}_{20}$ and $\nu=\tilde{a}_{10}/\tilde{a}_{20}$. The time for $\chi$ to change from 1 to 0 is the pump depletion time $T$. Thus,

$$F(\nu) \equiv \int_0^1 \frac{\mathrm{d}\chi}{\sqrt{1+\nu^2-\chi^2}\sqrt{1-\chi^2}} = \tilde{a}_{20}\frac{\sqrt{\omega_p\omega}}{2}T. \tag{19}$$

The pump depletion time measured from aPIC simulations is shown in Fig. 3. For the resonant case, the measured values show an excellent agreement with Eq. (19). The detuned case with the laser and plasma frequencies used in Fig. 2(b) was simulated for various $a_{10}/a_{20}$. Even though the pump depletion level was quite different from the resonant case for this detuning, the simulations show that the pump depletion time is not strongly dependent on it.

The pump depletion level is quite sensitive to $\delta\omega$ as seen in Fig. 2. Note that in Fig. 2 the pump depletion has been reduced by 40%, when the detuning is only 0.7%. Figure 4 shows the pump depletion level as a function of the detuning for various initial seed and pump intensities. For a very small initial seed, $\tilde{a}_{10}\ll\tilde{a}_{20}$, it is linearly dependent on the detuning. The scaling equation for the depletion level as a function of the detuning is

$$\frac{a_m}{\tilde{a}_{20}} = \frac{\delta\omega}{2\tilde{a}_{20}\sqrt{\omega_p\omega}}, \tag{20}$$

where $a_m$ means the minimum pump amplitude. It is found in Eq. (20) that suppression of the pump depletion is more severe for weaker pump. Figure 4 shows that even when the initial seed and pump ratio is not small $(a_{10}/a_{20}\sim 0.5)$, there is only a slight deviation from Eq. (20). The complete analytic solution of Eqs. (13) and (14) can be represented by Jacobi elliptic integrals.[12–14] The rigorous derivation of scaling equation (20) from the full analytic solution is under study.

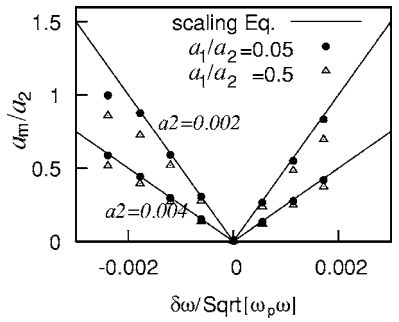


FIG. 4. Pump depletion as a function of the detuning $\delta\omega$ and the initial pump amplitude: the upper curve is for $a_2=0.002$ and the lower one is for $a_2=0.004$. The solid lines are from scaling equation (20) and the circles and triangles are from aPIC simulations.

Related with the sensitivity of RBS to the frequency detuning, a comment can be made on the effect of plasma temperature. The Langmuir wave frequency is determined by $\omega_{\mathrm{Langmuir}}=\omega_p+1.5k^2T_e/m_e\omega_p$, where the first term is the cold plasma frequency and the second one represents the thermal frequency shift. Though the thermal shift is negligible in many cases, it can be an important factor in RBS system due to the sensitivity of RBS to the frequency change. For a typical plasma temperature 10 eV, plasma density $n_p=1.38\times10^{19}$ cm$^{-3}$, and the wavelengths 1.0 and 0.9 $\mu$m for the seed and pump respectively, the thermal shift divided by $\omega_p$ is $1.5k^2T_e/m_e\omega_p^2=0.01$. This is large enough to make a great reduction in the pump depletion level.

## IV. SUMMARY

Raman backscattering in an infinite homogeneous system was investigated by three-wave fluid and averaged PIC simulations. The conventional periodic condition in the electrostatic potential was found to be significantly erroneous in the simulations of Raman backscattering. A correct boundary condition for the dc component of the electric field was presented. The aPIC simulations with the modified boundary condition showed an excellent agreement between the fluid and aPIC models. From simulations and analytic theory, we observed that the pump depletion time is governed dominantly by the initial seed and pump ratio $(a_1/a_2)$ and it is not so sensitive to the detuning between the three waves. On the other hand, the detuning is more important in determining the pump depletion level than $\tilde{a}_{10}/\tilde{a}_{20}$. In homogeneous cases, even a very small detuning, for example $\delta\omega/\omega_p<0.01$, can lead to a significant deterioration in the pump depletion level. We presented the comparison between the analytic formula and aPIC simulations for the pump depletion time and level. The sensitivity of RBS to the small detuning implies that a careful attention should be paid for example in determining plasma density from Raman (backward) spectroscopy.

## ACKNOWLEDGMENTS

This work was financially supported by the Creative Research Initiatives program/KOSEF of Korea Ministry of Science and Technology.

[1] C. I. Moore, A. Ting, K. Krushelnick, E. Esarey, R. F. Hubbard, B. Hafizi, H. R. Burris, C. Manka, and P. Sprangle, Phys. Rev. Lett. **79**, 3909 (1997).
[2] N. Hafz, M. S. Hur, G. H. Kim, C. Kim, I. S. Ko, H. Suk, Phys. Rev. E **73**, 016405 (2006).
[3] Z. Najmudin, R. Allott, F. Amiranoff, E. L. Clark, C. N. Danson, Daniel F. Gordon, C. Joshi, K. Krushelnick, V. Malka, D. Neely, M. R. Salvati, M. I. K. Santala, M. Tatarakis, and A. E. Dangor, IEEE Trans. Plasma Sci. **28**, 1122 (2000).
[4] H. X. Vu, D. F. DuBois, and B. Bezzerides, Phys. Rev. Lett. **86**, 4306 (2001); Phys. Plasmas **9**, 1745 (2002).

[5]S. Brunner and E. J. Valeo, Phys. Rev. Lett. **93**, 145003 (2004).
[6]V. M. Malkin, G. Shvets, and N. J. Fisch, Phys. Rev. Lett. **82**, 4448 (1990); Phys. Plasmas **7**, 2232 (2000).
[7]Y. Ping, W. Cheng, S. Suckewer, D. S. Clark, and N. Fisch, Phys. Rev. Lett. **92**, 175007 (2004).
[8]W. Cheng, Y. Avitzour, Y. Ping, S. Suckewer, N. J. Fisch, M. S. Hur, and J. S. Wurtele, Phys. Rev. Lett. **94**, 045003 (2005).
[9]M. S. Hur, R. R. Lindberg, A. E. Charman, J. S. Wurtele, and H. Suk, Phys. Rev. Lett. **95**, 115003 (2005).
[10]M. S. Hur, I. Hwang, and H. Suk, J. Korean Phys. Soc. **47**, 625 (2005).
[11]M. S. Hur, G. Penn, J. S. Wurtele, and R. Lindberg, Phys. Plasmas **11**, 5204 (2004).
[12]D. J. Kaup, A. Reiman, and A. Bers, Rev. Mod. Phys. **51**, 275 (1979).
[13]J. A. Armstrong, N. Bloembergen, J. Ducuing, and P. S. Pershan, Phys. Rev. **127**, 1918 (1962).
[14]R. C. Davidson, *Methods in Nonlinear Plasma Theory Academic* (Academic, New York, 1972).
[15]D. S. Clark and N. J. Fisch, Phys. Plasmas **10**, 4848 (2003).
[16]A. A. Balakin, D. V. Kartashov, A. M. Kiselev, S. A. Skobelev, A. N. Stepanov, and G. M. Fraiman, JETP Lett. **80**, 12 (2004).
[17]C. J. McKinstrie and D. W. Forslund, Phys. Fluids **30**, 904 (1987).
[18]W. B. Mori, IEEE Trans. Plasma Sci. **PS-15**, 88 (1987).
[19]G. Shvets, J. S. Wurtele, and B. A. Shadwick, Phys. Plasmas **4**, 1872 (1997).
[20]G. Shvets, N. J. Fisch, A. Pukhov, and J. Meyer-ter-Vehn, Phys. Rev. Lett. **81**, 4879 (1998).